 CMC, vol.5, no.2, pp.79-97, 2007

Fourier Analysis of Mode Shapes of Damaged Beams

Kanchi Venkatesulu Reddy[1] **and Ranjan Ganguli**[2]

Abstract: This paper investigates the effect of damage on beams with fixed boundary conditions using Fourier analysis of the mode shapes in spatial domain. A finite element model is used to obtain the mode shapes of a damaged fixed-fixed beam. Then the damaged beams are studied using a spatial Fourier analysis. This approach contrasts with the typical time domain application of Fourier analysis for vibration problems. It is found that damage causes considerable change in the Fourier coefficients of the mode shapes. The Fourier coefficients, especially the higher harmonics, are found to be sensitive to both damage size and location and amplify the changes in the mode shape due to the damage. Therefore, we formulate a damage index in the form of a vector of Fourier coefficients which is robust and unique for a given damage size and damage location. The effect of noise in the mode shape data is considered and it is found that Fourier coefficients provide a useful indication of damage even in the presence of noise. Various damage levels are considered and it is found that higher modes are needed to detect small amount of damage.

Keyword: Beam, Damage Detection, Vibration Analysis.

Nomenclature

a_i, b_i	Fourier coefficients
A_i	a value of Fourier coefficient a_i, above undamaged value
$-A_i$	a value of Fourier coefficient a_i, below undamaged value
B_i	a value of Fourier coefficient b_i, above undamaged value
$-B_i$	a value of Fourier coefficient b_i, below undamaged value
D	continuum damage variable
E	Young's modulus
E_0	undamaged Young's modulus
I	area moment of inertia of the beam cross section
K	stiffness matrix
L	length of the beam
m	mass per unit length of the beam
M	mass matrix
n	number of dof in FEM model
p	period in spatial domain
q	vector of nodal dofs
$w(x,t)$	transverse displacement of the beam
W	modal transverse displacement
x	length measured along the axis of the beam
α	noise level
β_i	i^{th} root of frequency equation
ϕ	mode shape vector
η	linear transformation $\eta = \frac{2\pi x}{L}$
ρ	uniform mass density
ω	natural frequency

1 Introduction

Structural systems are susceptible to damage during their service due to many factors such as in-service loads, fatigue and environmental effects. If undetected at an early stage, these damages may lead to failure of critical components of the structure or the structural system as a whole, which can be very costly in terms of human life and property. Therefore, online monitoring of the health of the structural systems attracted civil, mechanical and aerospace engineers in recent years. Numerous Nondestructive Damage Detection (NDD) meth-

[1] Graduate Student,Dept. of Aerospace Engg., Indian Institute of Science, Bangalore 560012, India.

[2] Asst. Professor(ganguli@aero.iisc.ernet.in), corresponding author, Dept. of Aerospace Engg., Indian Institute of Science, Bangalore 560012, India.

ods have been proposed and developed using different experimental and theoretical techniques. Well known examples of such techniques are ultrasonics, radiography, magnetic particle, dye penetrant and eddy current techniques. However, these methods have been applied to small-scale systems or a specific portion of large structures (hence also called "local" NDD methods). Another requirement of the local methods is that the structure must be accessible. Since these local methods can be applied for detecting damage only on local scale, and that too to the accessible portions of the structure, alternative methods that can be applied to the entire structure, (called global NDD methods), are gaining acceptance. The established global methods include thermography and acoustic emission.

However, the global methods using dynamic response of the structure have also gained significant attention in the past two decades. The basic idea behind these vibration response based global methods is that the changes in physical properties of the structure such as mass, stiffness and damping causes a change in dynamic characteristics such as natural frequency, damping ratio and mode shape of the structure. Therefore, by measuring these damage indicators, one should be able to predict the changes in physical properties resulting from damage.

Depending on the specific parameter of interest, there exists three different classes of dynamic damage detection methods. The first class of damage detection methods include those methods which use changes in natural frequency for damage detection. The appealing feature of this class of methods is the ease in measuring the natural frequencies. Some of the works in this class of methods are due to Viola et al (2001). Salawu (1997) gives a state of art review of methods which use frequency changes for damage detection. However, these methods have at least two limitations for their practical applicability Jeong-Tae et al (2003).

a. Since frequency change depends on square root of stiffness change, the changes in frequency caused due to damage are small.

b. Environmental conditions such as temperature, and moisture content can easily alter the frequency of the structure.

The second class of dynamic damage detection methods include those methods which use changes in the damping ratio. The effect of debonding on modal damping of sandwich panels was investigated by Peroni et al (1991). They showed that the damage caused a slight increase in the damping coefficient for some modes. Lai and Young (1995) reported extensive work on damage detection in composite structures including the effect of high temperature and prolonged exposure to humidity. They showed that, while delamination decreases the natural frequency of the fundamental mode, it increases the damping. However, they concluded that change in the damping coefficient is an unreliable parameter to be a basis for damage detection.

The third class of dynamic damage detection methods consists of methods which use changes in mode shapes of the structure for damage detection. Extensive research has been done on using mode shape changes for damage detection. The appealing feature of this class of methods is that changes in mode shape are much more sensitive to local damage than changes in natural frequency Jeong-Tae et al (2003). Various methods in this class basically differ in terms of the methodology adopted for magnifying the changes in mode shape caused by damage. Rizos and Aspragathos (1990) looked at using the changes in the mode shapes for damage detection in beams by measuring displacements at two points. Wang and Deng (1999), Chang and Lien-Wen (2005) and Douka et al (2003), applied wavelet analysis for detecting the damage from mode shape changes. Some researchers, like Ratcliff and Bagaria (1998) and Yoon et al (2005) have looked at using algorithms such as the gapped polynomial to magnify changes in mode shapes due to damage. Pandey et al (1991) used the modal curvature to amplify the effect of damage. Damage detection using rotation mode shapes was considered by Abdo and Hori (2002). Some other works are due to Parloo et al (2003) and Ratcliff (1997). A detailed review of vibration-based NDD methods has been

provided by Dimarogonas (1996). However using mode shape changes also has some drawbacks as given below.

a. Damage being a local phenomenon may not significantly influence the mode shape of lower modes that are usually measured from the vibration test for large structures.

b. The extracted mode shapes are affected by the environmental noise from such sources as ambient loads and inconsistent sensor positions.

c. The number of sensors and choice of sensor co-ordinates may have a crucial effect on the accuracy of damage detection procedure.

However, in recent years major advances have been realized in the field of structural dynamics and mechanical vibration measurements. The introduction of Scanning Laser Doppler Vibrometers(SLDV) Khan et al (2000), has revolutionized the dynamic testing and analysis due to its advantages such as its fast scanning capability and its non-contacting feature. Mode shape measurement and data analysis methods have therefore became well developed and this enables to easily overcome the above said limitations.

A natural question that arises is that, "why do we need so many damage detection methods and why one more when we have numerous methods already ?". This is well answered by the recent round-robin study conducted by Farrar and Jauregui (1996). In this study, the relative performance of prominent vibration based NDD methods such as (1) changes in flexibility method Pandey and Biswas (1994), (2) mode shape curvature method Pandey et al (1991), (3) change in uniform flexibility shapes curvature method Zhang and Aktan (1995), (4) change in stiffness method Zimmerman and Kaou (1995) and (5) damage index method Stubbs (1992), are discussed. On the basis of 16 damage cases studied using numerical and experimental data, even the best performing algorithm identified in that study, failed to identify certain damage cases at certain damage locations. Hence though there exist numerous vibration based NDD methods, no single method was shown to be completely effective in all situations. It can also be noticed that most of the methods developed to date are primarily useful for detecting damages of large size. Also they adopt a two stage approach for damage detection. In the first stage the damage localized and in the second stage the damage size is determined or vice-versa. Therefore there is a need for development of a robust damage index which can be used for detection up to small damage levels and should uniquely identify both damage location and damage size in one stage.

In this work, the authors formulate a damage index in the form of a vector of Fourier coefficients obtained by spatial Fourier analysis of mode shapes of damaged beams. The rationale for the present work is as follows. Many important structures can be represented as a beam that is fixed or pinned at one or both ends. For such structures, the boundary conditions lead to a mode shape which satisfy the condition $w(x)|_{x=0} = w(x)|_{x=L} = 0$, where $w(x)$ is lateral displacement of the mode shape. One can therefore assume that the mode shape for such structures is a periodic function in the *spatial* domain with period p=*L*. Therefore, the mode shape can be expanded in a spatial Fourier series. Most often Fourier analysis is done in the time domain and it seems to the authors that no work has looked at spatial Fourier analysis of damaged beams in which Fourier coefficients are used to magnify the changes in mode shape caused by damage. In this study, we show that damage in a fixed-fixed beam leads to a substantial change in the spatial Fourier coefficients of mode shapes. These changes can be used to detect small damage levels even in presence of noise in the measurement.

2 Analytical model for mode shapes

The equation of motion of an Euler-Bernoulli beam is

$$EI(x)\frac{\partial^4 w(x,t)}{\partial x^4} + m(x)\frac{\partial^2 w(x,t)}{\partial t^2} = f(x,t) \qquad (1)$$

For a uniform beam we can obtain frequencies and mode shapes as an exact solution. Setting $f(x,t) = 0$ for free vibration and assuming $w(x,t)$

as, $w(x,t) = W(x)^{(i\omega t)}$, eq.(1) yields

$$\frac{d^4W}{dx^4} - \omega^2 \frac{m}{EI} W = 0 \tag{2}$$

The above is an ordinary differential equation of 4^{th} order in space. The general solution of this equation is of the form

$$W(x) = A\sin(\lambda x) + B\cos(\lambda x) + C\sinh(\lambda x) + D\cosh(\lambda x) \tag{3}$$

Where $\lambda = \left(\frac{m\omega^2}{EI}\right)^{1/4}$ and ω is natural frequency. Solving eq.(3) with appropriate boundary conditions gives the frequency equation. Substituting the roots of this frequency equation, $(\beta)_i, i = 1,2,.....n$, in $\lambda = \left(\frac{m\omega^2}{EI}\right)^{1/4}$, where $\lambda = \frac{\beta}{L}$, we obtain the i^{th} frequency. Substituting λ in eq.(3) gives the mode shape corresponding to the i^{th} mode.

3 Finite element model for mode shapes

Damage in a uniform beam leads to a reduction in stiffness at the damage location thereby making it non-uniform. For free vibration analysis of non-uniform beams the finite element method is used. The beam is discretized into a number of beam elements, with displacement and slope as nodal degrees of freedom and cubic interpolation functions.

For an n degree of freedom system, the equation of motion in discrete form is obtained after assembly of the element matrices and application of the boundary conditions.

$$\mathbf{M}\ddot{\mathbf{q}} + \mathbf{K}\mathbf{q} = 0 \tag{4}$$

Here $\mathbf{M}$ is the $n \times n$ mass matrix of the system, $\mathbf{K}$ is the $n \times n$ stiffness matrix of the system, $\mathbf{q}$ is the $n \times 1$ vector of nodal degrees of freedom. We seek a solution of the form $q = \Phi^{(i\omega t)}$, which results in the eigenvalue problem.

$$\mathbf{K}\Phi = \omega^2 \mathbf{M}\Phi \tag{5}$$

Solving this eigenvalue problem we get n eigenvalues which represent the n natural frequencies of the system. The associated eigenvectors along with shape functions give the mode shape corresponding to that mode.

4 Spatial Fourier analysis

As an example, consider the case of a beam fixed at both ends. The boundary condition for a fixed-fixed beam are given by

$$\begin{aligned} W(0) &= 0, \quad W(L) = 0, \\ \frac{dW(0)}{dx} &= 0, \quad \frac{dW(L)}{dx} = 0 \end{aligned} \tag{6}$$

Solving eq.(3) with these boundary conditions gives the frequency equation and equation for mode shape as eq.(7) and eq.(8) respectively.

$$\cos(\lambda L)\cosh(\lambda L) = 1 \tag{7}$$

The first, second and third roots of the transcendental equation eq.(7) which corresponds to first, second and third modes of vibration are obtained as 4.730040745, 7.853204624 and 10.995607838 respectively. Substituting this in eq.(8) gives the corresponding mode shapes as shown in the Fig. (1).

$$W(x) = \left\{\cos\left(\frac{\beta x}{L}\right) - \cosh\left(\frac{\beta x}{L}\right)\right\} - \left\{\frac{\cos(\beta) - \cosh(\beta)}{\sin(\beta) - \sinh(\beta)}\right\} \cdot \left\{\sin\left(\frac{\beta x}{L}\right) - \sinh\left(\frac{\beta x}{L}\right)\right\} \tag{8}$$

It can be observed from Fig.1 that $W(x)|_{x=0} = W(x)|_{x=L} = 0$. Hence the mode shapes are periodic in space(x) with period $p = L$. Since the mode shapes are periodic, they can be expressed in the form of Fourier series as in eq.9, taking the linear transformation $\eta = \frac{2\pi x}{L}$ which transforms the problem from $x \in [0,L]$ to $\eta \in [0,2\pi]$.

$$W(\eta) = a_0 + \sum_{i=1}^{m} \{a_i \cos(i\eta) + b_i \sin(i\eta)\} \qquad (9)$$

where $a_i, i = 0,1,2,....m$ and $b_j, j = 1,2,3,.....m$ are Fourier coefficients. To obtain Fourier coefficients for the exact and finite element mode shapes, they are uniformly sampled at a number of discrete points. The mode shapes are normalized with respect to highest value. By fitting a curve similar to that in eq.(9), one gets the Fourier coefficients.

5 Numerical results

Consider a beam with the following properties; E=200 GPa, I=2000 mm^4, A=240 mm^2, ρ=7800 kg/m^3 and L=600 mm. The natural frequencies and mode shapes are computed using the methodology described in the previous section. Fig. 1 shows the first three mode shapes for the selected example. The beam is divided into 20 finite elements of equal length. Numerical results for the FEM analysis are validated with the exact solutions.

5.1 Fourier analysis of undamaged beam

The Fourier analysis of different mode shapes of an undamaged fixed-fixed beam are considered in this section. Fourier coefficients for mode 1, 2 and 3 of an undamaged fixed-fixed beam obtained using analytical as well as FE model are given in Tab.1, 2 and 3, respectively. The FE solution matches exactly with the analytical solution to five decimal places. Hence the developed FE model represents the mode shape with sufficiently good accuracy. From Tab.1 and Tab.3 it can be observed that, since all b_j, j=1,2,...m, are zero, the first and third mode shapes are cosine functions. Also from Tab.2 it can be observed that, since all a_i, i=1,2,...n, are zero, the second mode shape is a sine function. In general it is observed that all odd number of mode shapes are cosine functions and all even number of mode shapes are sine functions. Furthermore, it is observed that the steady and first harmonics are most dominant and other harmonics decrease rapidly for higher harmonics as shown by ε in the Tab.1 through Tab.3. Here ε is a small number of magnitude 0.1.

Table 1: Fourier coefficients for first mode of fixed-fixed beam

Coefficient	Analytical Value	Normalized Value	Order of magnitude	FE Value
a_0	0.52316	1.00000	1	0.52316
a_1	-0.49505	-0.96420	1	-0.49505
b_1	0.00000			
a_2	-0.02143	-0.04097	ε^2	-0.02143
b_2	0.00000			
a_3	-0.00416	-0.00796	ε^2	-0.00416
b_3	0.00000			
a_4	-0.00131	-0.00251	ε^3	-0.00131
b_4	0.00000			
a_5	-0.00054	-0.00103	ε^3	-0.00054
b_5	0.00000			
a_6	-0.00026	-0.00049	ε^3	-0.00026
b_6	0.00000			
a_7	-0.00014	-0.00027	ε^4	-0.00014
b_7	0.00000			
a_8	-0.00008	-0.00016	ε^4	-0.00008
b_8	0.00000			
a_9	-0.00005	-0.00010	ε^4	-0.00005
b_9	0.00000			
a_{10}	-0.00003	-0.00007	ε^4	-0.00003
b_{10}	0.00000			

5.2 Fourier analysis of damaged beam

Any structural damage can be modelled by appropriately reducing the stiffness of the cross section at the location of the damage using the continuum damage variable $D = 1 - \frac{E}{E_0}$, which varies from 0 for an undamaged case($E = E_0$) to 1 for complete damage($E = 0$). A percent damage value of D is used in this paper, Where $D = 0$ percent stands for no damage and $D = 100$ stands for complete damage. For numerical results in this paper, a maximum value of D of 50% is considered.

The FE model developed is used to examine the impact of damage in the beam on the Fourier coefficients of the mode shapes. The Fourier coefficients, for damage locations varying from element number 1 to 20 and damage size as characterized by D, varying from 0 to 50% are computed using the FE model developed. Fig.3 through Fig.5 show the variation of different Fourier coefficients for first three modes of a fixed-fixed beam for

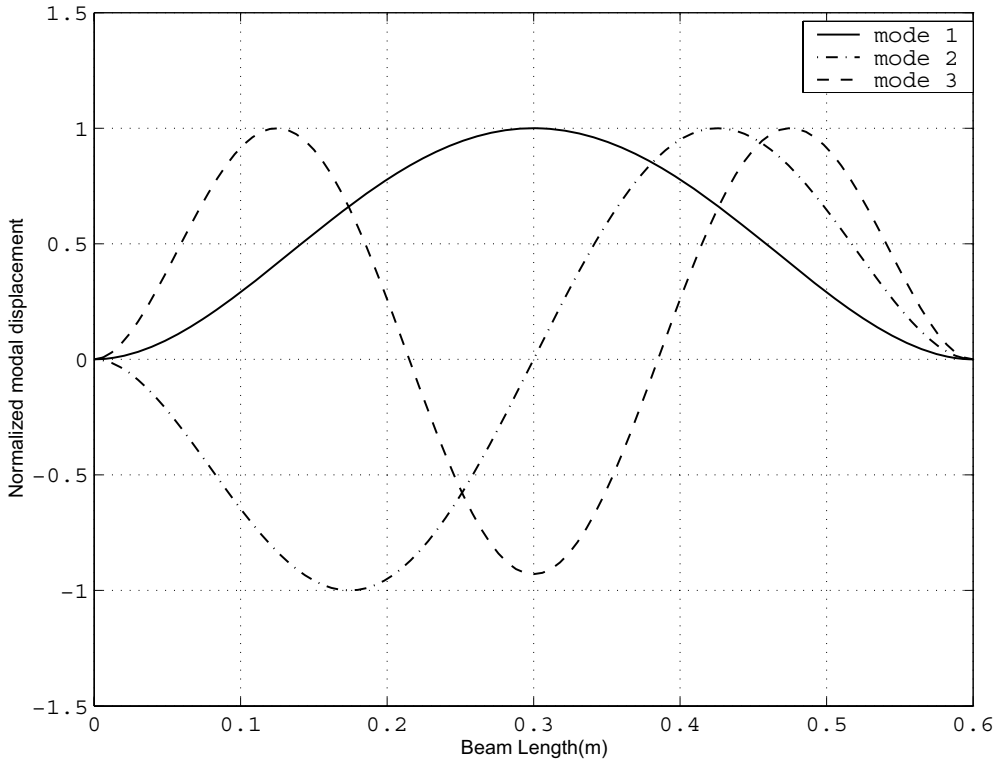

Figure 1: First three mode shapes of an undamaged fixed-fixed beamSome functions of x

different damage size and damage locations. It is found that Fourier coefficients are sensitive to damage in the beam. In particular, the higher harmonics show the considerable influence of damage location. In addition, there is a clear increase in the magnitude of all coefficients as damage increases from 0 to 50 percent. For mode 1 and mode 3, the a_j coefficients are symmetric and b_j are antisymmetric. For mode 2, the a_j coefficients are antisymmetric and b_j are symmetric. In general for all odd number of modes a_j are symmetric and b_j are antisymmetric and for all even number of modes a_j are antisymmetric and b_j are symmetric. The antisymmetric coefficients are useful for locating damage between two symmetric locations of the beam(for example $x = 0.2L$ and $x = 0.8L$), where the symmetric coefficients show the same Fourier coefficients. Thus at least one symmetric and one antisymmetric mode are needed to uniquely locate damage in fixed-fixed beam.

Also it can be noted that the Fourier coefficients which are zero for undamaged beam (b_j for mode 1 and mode 3, a_j for mode 2) in Tab.1 through Tab.3, now attain non zero values due to the presence of damage. This non-zero values increase monotonically with damage size. The occurrence of sine harmonics in the Fourier coefficients of mode 1 and 3 and cosine harmonics in the Fourier coefficients of mode 2 are therefore indication of damage in the beam. It has also been found that each location-damage size pair has an unique set of sensitive Fourier coefficients, which can be considered as an unique damage index for that particular damage location and damage size. This will be demonstrated in detail in later sections in the paper.

6 Numerical experiment

Since detection of damage sizes of less than 50% is of more engineering interest, we have considered damage sizes 50%, 40%, 30%, 20%, 15% and 10% and damage location varying from element number 1 through 20. In order to simulate the experimental noise and errors in measurements and models, we have added noise to the

Table 2: Fourier coefficients for second mode of fixed-fixed beam

.

Coefficient	Analytical Value	Normalized Value	Order of magnitude	FE Value
a_0	-0.00000			
a_1	0.00000			
b_1	-0.91494	1.00000	1	-0.91494
a_2	-0.00000			
b_2	0.19439	-0.21246	ε	0.19439
a_3	-0.00000			
b_3	0.05033	-0.05501	ε	0.05033
a_4	-0.00000			
b_4	0.02079	-0.02272	ε^2	0.02079
a_5	-0.00000			
b_5	0.01058	-0.01157	ε^2	0.01058
a_6	-0.00000			
b_6	0.00611	-0.00668	ε^2	0.00611
a_7	-0.00000			
b_7	-0.00385	-0.00420	ε^3	-0.00385
a_8	-0.00000			
b_8	-0.00257	-0.00281	ε^3	-0.00257
a_9	0.00000			
b_9	0.00181	-0.00198	ε^3	0.00181
a_{10}	-0.00000			
b_{10}	0.00132	-0.00144	ε^3	0.00132

Table 3: Fourier coefficients for third mode of fixed-fixed beam

.

Coefficient	Analytical Value	Normalized Value	Order of magnitude	FE Value
a_0	0.24056	-0.35294	ε	0.24055
a_1	0.53853	-0.79013	1	0.53852
b_1	0.00000			
a_2	-0.68157	1.00000	1	-0.68155
b_2	-0.00000			
a_3	-0.06303	-0.09247	ε	-0.06303
b_3	-0.00000			
a_4	-0.01832	-0.02688	ε^2	-0.01832
b_4	0.00000			
a_5	-0.00735	-0.01079	ε^2	-0.00735
b_5	0.00000			
a_6	-0.00353	-0.00518	ε^2	-0.00353
b_6	0.00000			
a_7	-0.00191	-0.00280	ε^3	-0.00191
b_7	-0.00000			
a_8	-0.00113	-0.00165	ε^3	-0.00113
b_8	-0.00000			
a_9	-0.00071	-0.00104	ε^3	-0.00071
b_9	-0.00000			
a_{10}	-0.00047	-0.00069	ε^3	-0.00047
b_{10}	-0.00000			

FE mode shape according to eq.(10). Here α is a measure of noise level and is taken to be 0.01 and the function rand() generates random numbers varying from -1 to +1. Fig. 2 shows a sample ideal and noisy mode shape.

$$\Phi^{(noisy)}(i) = \Phi^{(ideal)}(i) + \alpha * rand() \tag{10}$$

One thousand noisy mode shapes are created for undamaged and damaged beam using eq.(10), and Fourier coefficients are obtained as explained in section 4. Here Φ is the vector containing the mode shapes. From these thousand cases, two cases with maximum deviation above and maximum deviation below the ideal(noise free) results are selected for both the undamaged beam and the damaged beam. Fig.6 through Fig.8 show the variation of Fourier Coefficients in presence of noise for first, second and third modes of a fixed-fixed beam for undamaged and a selected damage size of 40%. It is clear from these figures and as shown in the Fig.9 as an example that there is an undamaged zone between the two horizontal lines where the Fourier coefficients of undamaged beam lie. Similarly there is a damaged zone where the Fourier coefficients of the damaged beam lie. The pattern classification between the damaged and undamaged beams can be made for damage location where the 'undamaged' and 'damaged' zones do not intersect and are unique. The undamaged and damaged cases are compared to find the Fourier coefficients which are out of the undamaged noise band. For example damage at element 1, 9, 10, 11, 12 and 20 cause changes in a_2 which lie outside the undamaged band. This observation leads to the results in Tab.5 in the mode 1 column. For each damage size and damage location pair thus obtained Fourier coefficients are the ones which undergo considerable change due to presence of damage. Tab.4 through Tab.9 gives the vector of sensitive Fourier coefficients for each damage size and damage location pair which is the damage index. In these tables capital letters A, B are used for the Fourier coefficients to indicate that these coefficients are outside the noise band for the undamaged beam and therefore useful for damage detection. For

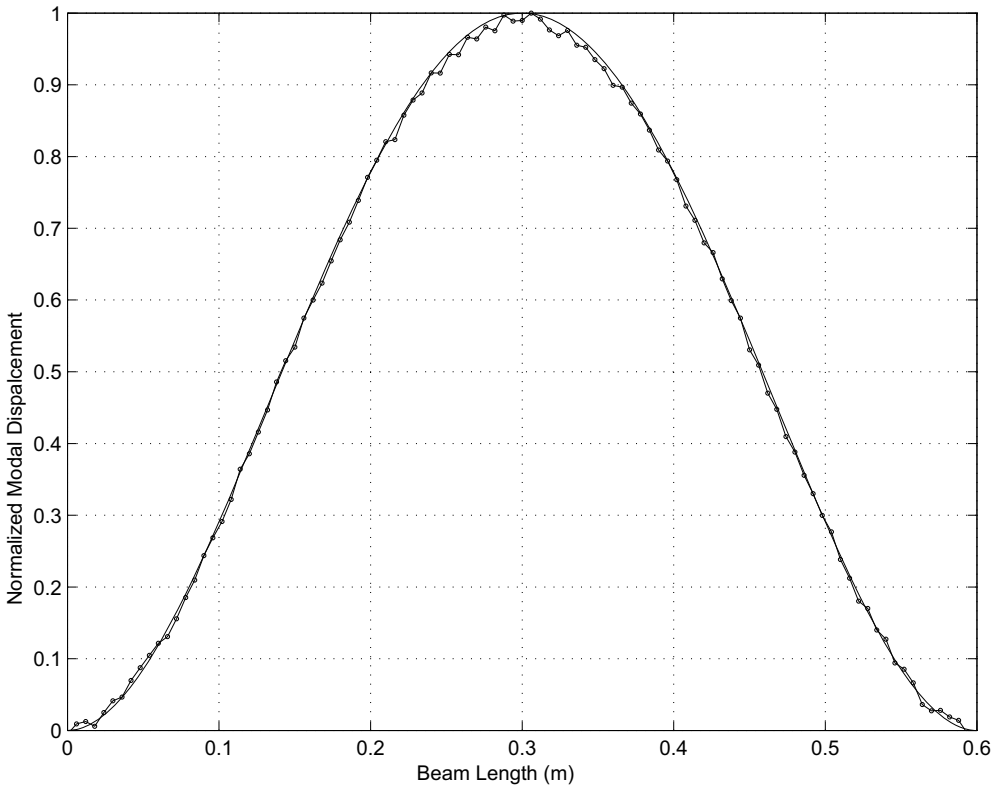

Figure 2: Noisy first mode shape of an undamaged fixed-fixed beam

Table 4: Fourier Coefficients above noise level for 50% damage

Damage Location	Mode 1	Mode 2
1	$A_0, B_1, -A_2, -A_3$	$A_0, -A_1, A_2, -B_2, A_3, A_4$
2	B_1	$A_0, -A_1, A_2$
3	$-B_2$	
4		$-A_0, -A_1, A_2, -B_2, A_3$
5		$-A_0, -A_1, B_1, A_2, -B_2, A_3, B_3, -A_4$
6	B_1	$-A_1, B_1, A_2, -B_2, -A_3, B_3, -A_4, -B_4$
7	$B_1, -B_2$	$A_0, -A_1, B_1, A_2, B_2, -A_3, -B_4$
8	$B_1, -B_2$	$A_0, B_1, B_2, -A_3, -B_3, A_4$
9	$B_1, A_2, -B_2$	$A_0, B_1, -A_2, B_2, -B_3$
10	$-A_0, A_2$	$A_0, -A_2$
11	$-A_0, A_2$	$-A_0, A_2$
12	$-B_1, A_2, B_2$	$-A_0, B_1, A_2, B_2, -B_3$
13	$-B_1, B_2$	$-A_0, B_1, B_2, A_3, -B_3, -A_4$
14	$-B_1, B_2$	$-A_0, A_1, B_1, -A_2, B_2, A_3, -B_4$
15	$-B_1$	$A_1, B_1, -A_2, -B_2, A_3, B_3, A_4, -B_4$
16		$A_0, A_1, B_1, -A_2, -B_2, -A_3, B_3, A_4$
17		$A_0, A_1, -A_2, -B_2, -A_3$
18	B_2	
19	$-B_1$	$-A_0, A_1, -A_2$
20	$A_0, -B_1, -A_2, -A_3$	$-A_0, A_1, -A_2, -B_2, -A_3, -A_4$

Table 5: Fourier Coefficients above noise level for 40% damage

Damage Location	Mode 1	Mode 2	Mode 3
1	$A_0, B_1, -A_2$	$A_0, -A_1, A_2, -B_2, A_3$	$A_1, -B_1, A_2, B_2, -A_3, -A_4$
2	B_1	$A_0, -A_1, A_2$	$-B_1$
3			$B_2, -A_3$
4		$-A_0, -A_1, A_2, -B_2$	$-A_0, -A_1, A_2, B_2, -A_3, -B_3, -B_4, A_5$
5		$-A_0, -A_1, B_1, A_2, -B_2, B_3$	$-A_0, -A_1, -B_1, A_2, B_2, -B_3, A_4, -B_4, A_5, B_5$
6		$-A_1, B_1, A_2, -B_2, B_3$	$-A_0, -B_1, A_3, -B_3, A_4, B_4, B_5$
7	$B_1, -B_2$	$A_0, -A_1, B_1, A_2, B_2, -A_3$	$-B_1, A_3$
8	$B_1, -B_2$	$A_0, B_2, -A_3, -B_3$	$B_1, B_2, -B_3$
9	$B_1, A_2, -B_2$	$A_0, -A_2, -B_3$	$-A_0, -A_1, B_1, A_2, B_2, A_3, -B_3, B_4, -B_5$
10	$-A_0, A_2$	$A_0, -A_2$	$-A_1, B_1, B_2, A_3, -B_3, -A_4, B_4, A_5, -B_5$
11	$-A_0, A_2$	$-A_0, A_2$	$-A_1, -B_1, -B_2, A_3, B_3, -A_4, -B_4, A_5, B_5$
12	$-B_1, A_2, B_2$	$-A_0, A_2, -B_3$	$-A_0, -A_1, -B_1, A_2, -B_2, A_3, B_3, -B_4, B_5$
13	$-B_1, B_2$	$-A_0, B_2, A_3, -B_3$	$-B_1, -B_2, B_3$
14	$-B_1, B_2$	$-A_0, A_1, B_1, -A_2, B_2, A_3$	B_1, A_3
15		$A_1, B_1, -A_2, -B_2, B_3$	$-A_0, B_1, A_3, B_3, A_4, -B_4, -B_5$
16		$A_0, A_1, B_1, -A_2, -B_2, B_3$	$-A_0, -A_1, B_1, A_2, -B_2, B_3, A_4, B_4, A_5, -B_5$
17		$A_0, A_1, -A_2, -B_2$	$-A_0, -A_1, A_2, -B_2, -A_3, B_3, B_4, A_5$
18			$-B_2, -A_3$
19	$-B_1$	$-A_0, A_1, -A_2$	B_1
20	$A_0, -B_1, -A_2$	$-A_0, A_1, -A_2, -B_2, -A_3$	$A_1, B_1, A_2, -B_2, -A_3, -A_4$

example, in Tab.6 it is mentioned that damage in element 1 causes measurable changes in Fourier coefficients B_1 and -A_2 which can be seen from Fig.6. The negative sign before A_2 points to a decrease relative to the undamaged case. Note that damage in element 20 causes measurable changes in -A_1 and -A_2 and both have negative signs. Thus the antisymmetric coefficients such as b_1 are needed to differentiate between damage in element 1 and element 20. Note that using mode 1 alone does not allow differentiation between many of the elements. However, the differentiation between different elements becomes possible using higher modes.

It is clear from Tab.4 through Tab.9 that more modes are needed to isolate damage as the size of damage decreases. Thus 50% damage can be isolated using the Fourier coefficients of only the first two modes, while the first three modes are needed for 40%, 30% and 20% damage. Damage size of 15% needs the first five modes and damage of 10% is harder to detect and requires the Fourier coefficients of the first six modes. In general, lower modes such as first three can be measured with good accuracy. Hence we can say that the proposed method can be effectively applied for detecting and isolating damage of size greater than 20%, though it can be applied to even smaller damages. Another interesting result to note from Tab.4 through tab.9 is that, for a given mode, the Fourier coefficients at lower damage level are a subset of those at higher damage level. For example, in Tab.9 damage of 10% at element 1 leads to the signature -A_1, A_2 for mode 2. For 15% damage the signature is -A_1, A_2, -B_2. For 20% damage the signature is -A_1, A_2, -B_2. For 30% damage the signature is A_0, -A_1, A_2, -B_2, A_3. For 40% damage it is A_0, -A_1, A_2, -B_2, A_3 and for 50% damage it is A_0, -A_1, A_2, -B_2, A_3, A_4. Thus we see that as the damage size at element 1 increases from 10% to 50%, new Fourier coefficients become measurable thus requiring less number of modes for damage isolation. The changes in the Fourier coefficients due to damage is well above the considered noise level. Hence these can be considered as the unique signatures of each location and damage pair. In other words, these unique signatures can be used for detecting damage location and damage size. Tab.4 - 9 can be used to develop pattern recognition algorithm for

Table 6: Fourier Coefficients above noise level for 30% damage

Damage Location	Mode 1	Mode 2	Mode 3
1	$B_1, -A_2$	$A_0, -A_1, A_2, -B_2, A_3$	$A_1, -B_1, B_2, -A_3, -A_4$
2	B_1	$A_0, -A_1$	
3			B_2
4		$-A_0, A_2$	$-A_1, A_2, B_2, -A_3, -B_3, -B_4$
5		$-A_0, -A_1, A_2, -B_2$	$-A_1, -B_1, A_2, B_2, -B_3, A_4$
6		$-A_1, B_1, A_2$	$-B_1, A_3, -B_3, A_4$
7	B_1	$A_0, -A_1, A_2, -A_3$	$-B_1, A_3$
8	B_1	$A_0, B_2, -A_3, -B_3$	B_1, B_2
9	B_1	$A_0, -A_2, -B_3$	$-A_1, B_1, A_2, B_2, A_3, -B_3$
10	A_2		$-A_1, B_1, B_2, A_3, -B_3, -A4$
11	A_2		$-A_1, -B_1, -B_2, A_3, B_3, -A4$
12	$-B_1$	$-A_0, A_2, -B_3$	$-A_1, -B_1, A_2, -B_2, A_3, B_3$
13	$-B_1$	$-A_0, B_2, A_3, -B_3$	$-B_1, -B_2$
14	$-B_1$	$-A_0, A_1, -A_2, A_3$	B_1, A_3
15		$A_1, B_1, -A_2$	B_1, A_3, B_3, A_4
16		$A_0, A_1, -A_2, -B_2$	$-A_1, B_1, A_2, -B_2, B_3, A_4$
17		$A_0, -A_2$	$-A_1, A_2, -B_2, -A_3, B_3, B_4$
18			$-B_2$
19	$-B_1$	$-A_0, A_1$	
20	$-B_1, -A_2$	$-A_0, A_1, -A_2, -B_2, -A_3$	$A_1, B_1, -B_2, -A_3, -A_4$

Table 7: Fourier Coefficients above noise level for 20% damage

Damage Location	Mode 1	Mode 2	Mode 3
1	B_1	$-A_1, A_2, -B_2$	$-B_1, B_2, -A_3$
2	B_1		
3			B_2
4			$B_2, -A_3$
5		A_2	$-B_1, B_2, -B_3$
6		A_2	$-B_1, A_3, -B_3$
7		A_2	$-B_1$
8	B_1	A_0	
9		$A_0, -A_2$	$B_1, B_2, -B_3$
10			$B_2, A_3, -B_3$
11			$-B_2, A_3, B_3$
12		$-A_0, A_2$	$-B_1, -B_2, B_3$
13	$-B_1$	$-A_0$	
14		$-A_2$	B_1
15		$-A_2$	B_1, A_3, B_3
16		$-A_2$	$B_1, -B_2, B_3$
17			$-B_2, -A_3$
18			$-B_2$
19	$-B_1$		
20	$-B_1$	$A_1, -A_2, -B_2$	$B_1, -B_2, -A_3$

Table 8: Fourier Coefficients above noise level for 15% damage

Damage Location	Mode 1	Mode 2	Mode 3	Mode 4	Mode 5
1	B_1	$-A_1, A_2, -B_2$	$-B_1, B_2$	$-A_2, A_3, -B_3$	$-B_1, -B_2, B_3$
2					B_3
3			B_2	$-A_2, A_3, -B_3$	$-A_1, -B_2, A_3, B_3$
4			B_2	$-A_2, A_3$	$-B_2, B_3$
5		A_2	$-B_1, B_2, -B_3$	$A_1, -A_2$	
6		A_2	$-B_1$		$-A_2, -B_2, A_3, B_3, -B_4$
7				$-A_1, A_3$	$-B_2, B_3, A_4, -B_4$
8		A_0		$-A_2, A_3, -A_4$	$-B_2, A_4$
9			$B_1, B_2, -B_3$	$A_1, -A_2, -B_4$	
10			A_3	$A_1, -A_3$	$B_2, B_3, A_4, -B_4$
11			A_3	$-A_1, A_3$	$-B_2, -B_3, A_4, B_4$
12			$-B_1, -B_2, B_3$	$-A_1, A_2, -B_4$	
13		$-A_0$		$A_2, -A_3, A_4$	B_2, A_4
14				$A_1, -A_3$	$B_2, -B_3, A_4, B_4$
15		$-A_2$	B_1		$-A_2, B_2, A_3, -B_3, B_4$
16		$-A_2$	$B_1, -B_2, B_3$	$-A_1, A_2$	
17			$-B_2$	$A_2, -A_3$	$B_2, -B_3$
18			$-B_2$	$A_2, -A_3, -B_3$	$-A_1, B_2, A_3, -B_3$
19					$-B_3$
20	$-B_1$	$A_1, -A_2, -B_2$	$B_1, -B_2$	$A_2, -A_3, -B_3$	$B_1, B_2, -B_3$

Table 9: Fourier Coefficients above noise level for 10% damage

Damage Location	Mode 1	Mode 2	Mode 3	Mode 4	Mode 5	Mode 6
1	B_1	$-A_1, A_2$	$-B_1, B_2$	A_3	$-B_2, B_3$	$A3, -A_4$
2						$A3, -A_4$
3				$-A_2, A_3$	$-B_2, B_3$	$A3, -A_4$
4			B_2	$-A_2, A_3$	$-B_2, B_3$	
5			B_2			$A3, -A_4, B_4$
6			$-B_1$		$B_3, -B_4$	$-A2, A_3, -A_4$
7				A_3	$-B_2, B_3, -B_4$	
8				A_3	$-B_2$	$-A_4$
9			B_2	A_1		$-B_4$
10			A_3		B_2, A_4	$-A2, A_4$
11			A_3		$-B_2, A_4$	$A2, -A_4$
12			$-B_2$	$-A_1$		$-B_4$
13				$-A_3$	B_2	A_4
14				$-A_3$	$B_2, -B_3, B_4$	
15			B_1		$-B_3, B_4$	$A2, -A_3, A_4$
16			$-B_2$			$-A3, A_4, B_4$
17			$-B_2$	$A_2, -A_3$	$B_2, -B_3$	
18				$A_2, -A_3$	$B_2, -B_3$	$-A3, A_4$
19						$-A3, A_4$
20	$-B_1$	$A_1, -A_2$	$B_1, -B_2$	$-A_3$	$B_2, -B_3$	$-A3, A_4$

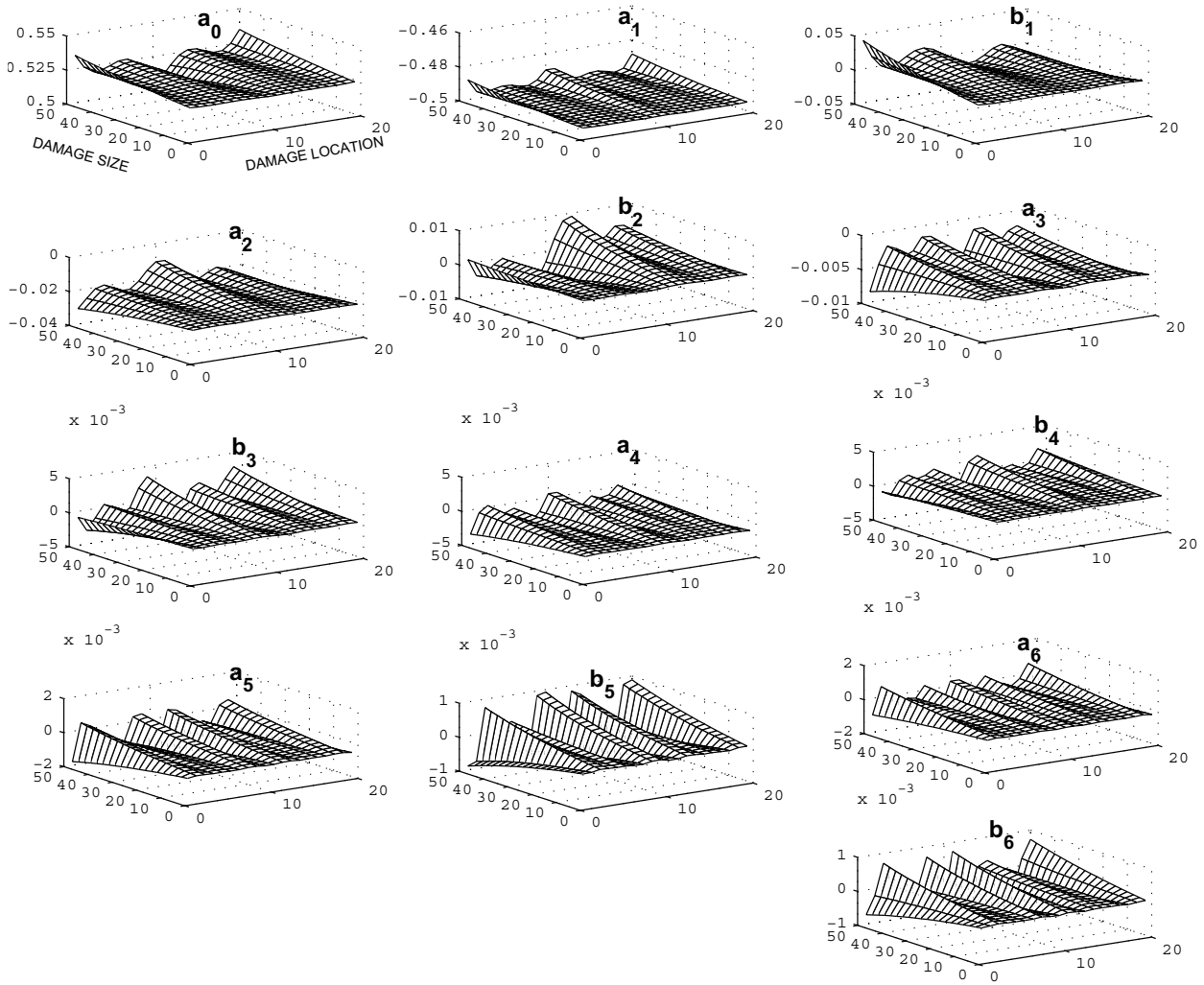

Figure 3: Variation of Fourier coefficients for the 1^{st} mode of a fixed-fixed beam

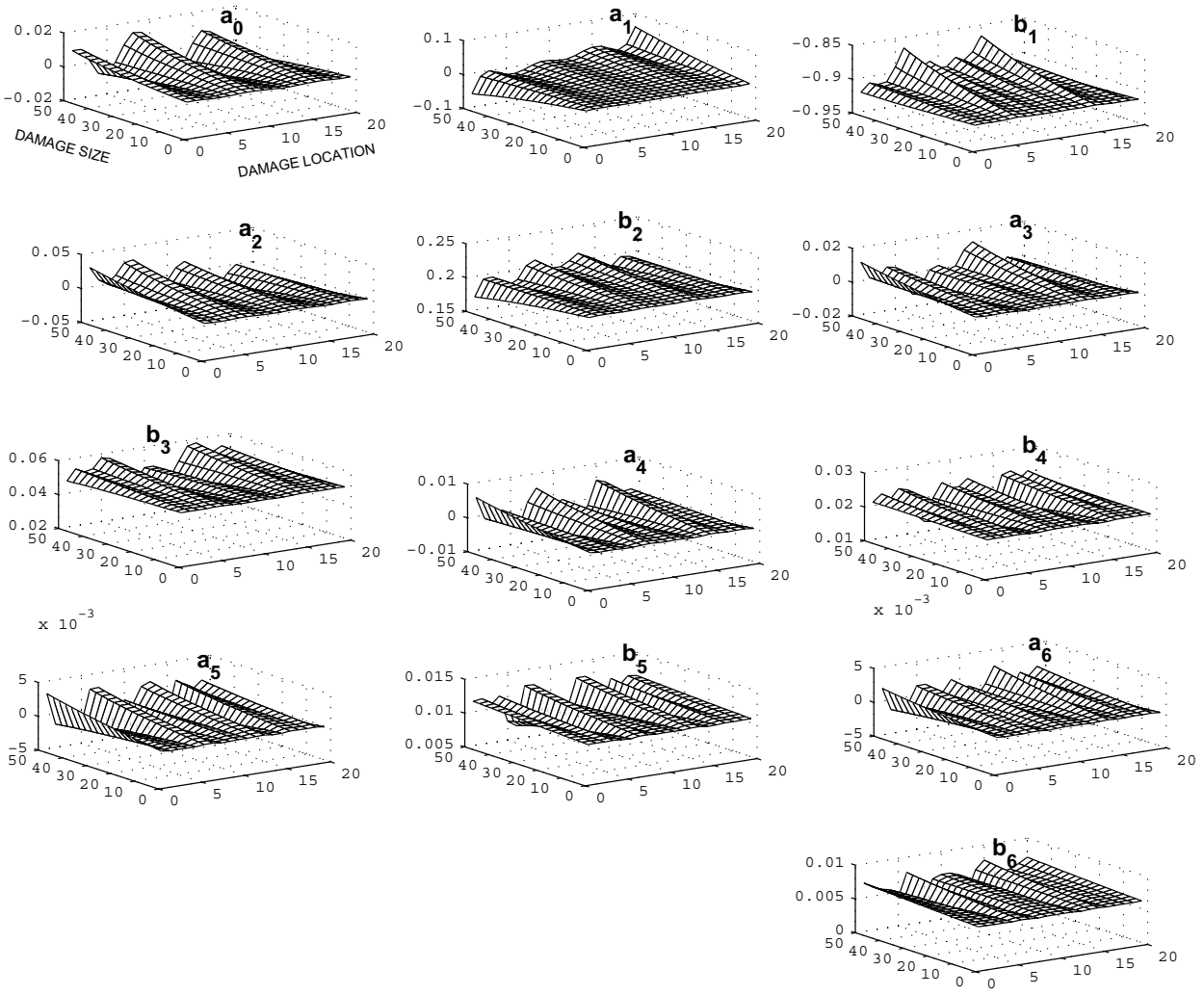

Figure 4: Variation of Fourier coefficients for the 2^{nd} mode of a fixed-fixed beam

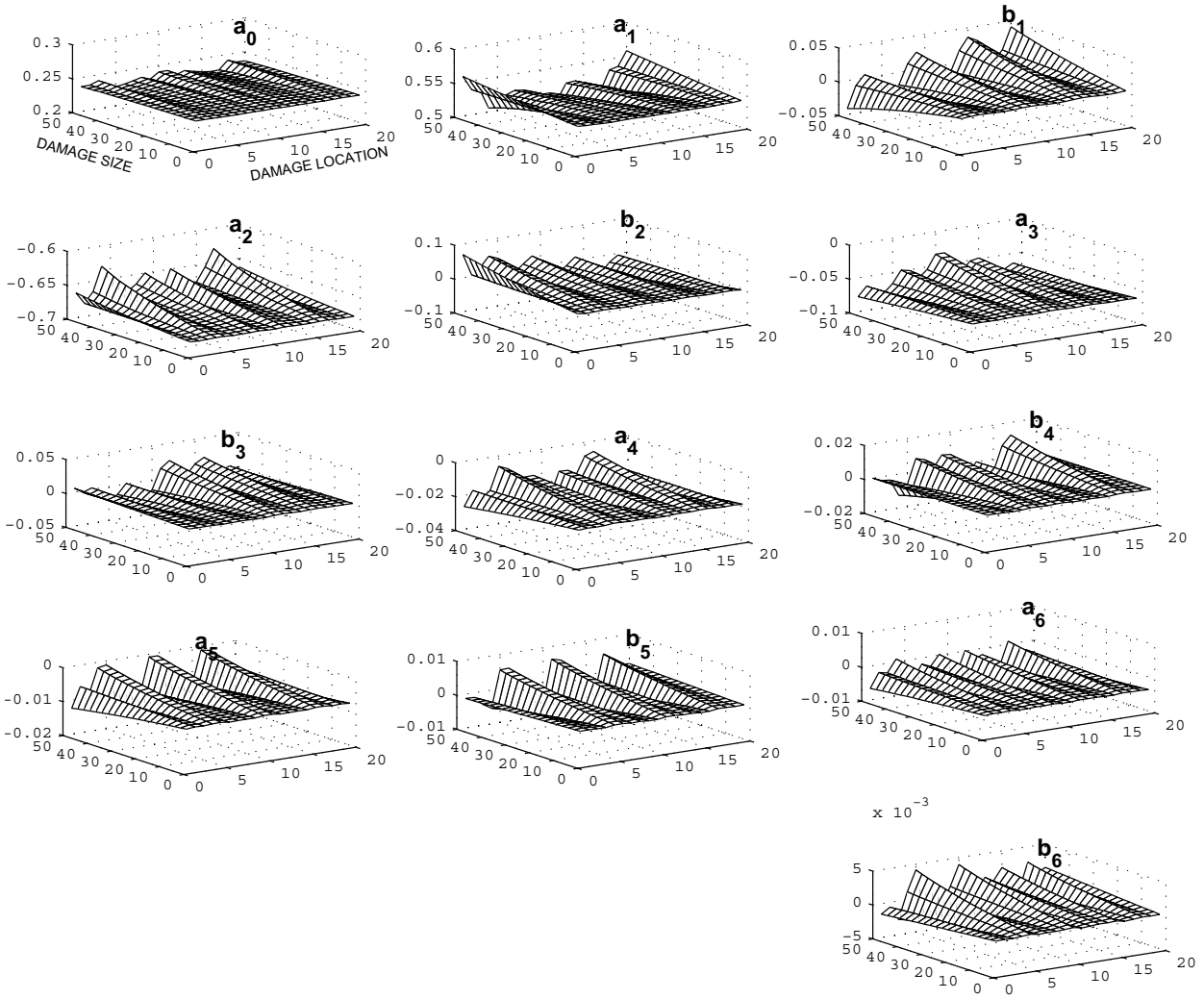

Figure 5: Variation of Fourier coefficients for the 3^{rd} mode of a fixed-fixed beam

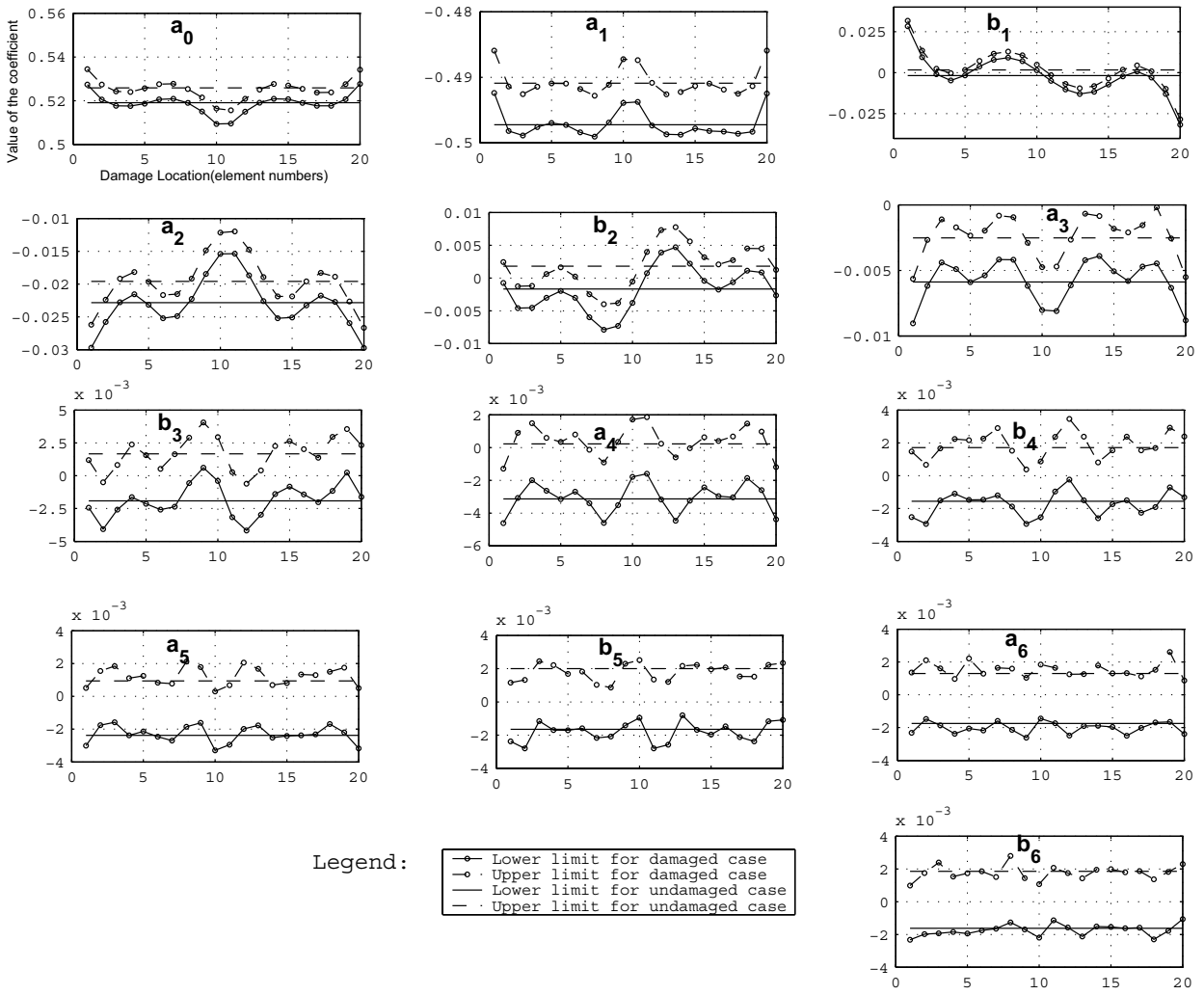

Figure 6: Variation of Fourier coefficients in presence of noise for 1^{st} mode of fixed-fixed beam for undamaged and damage size of 40%

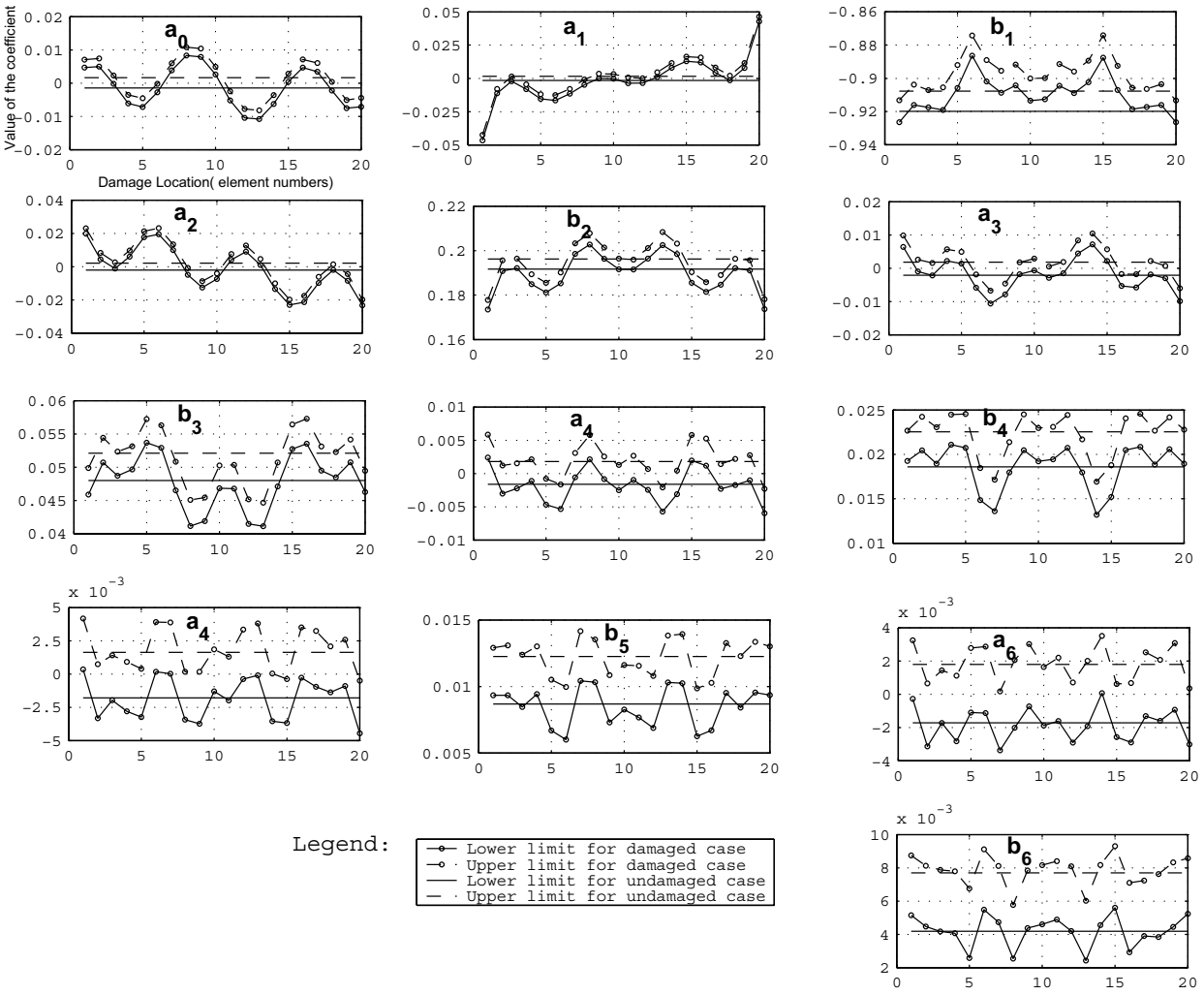

Figure 7: Variation of Fourier coefficients in presence of noise for 2^{nd} mode of fixed-fixed beam for undamaged and damage size of 40%

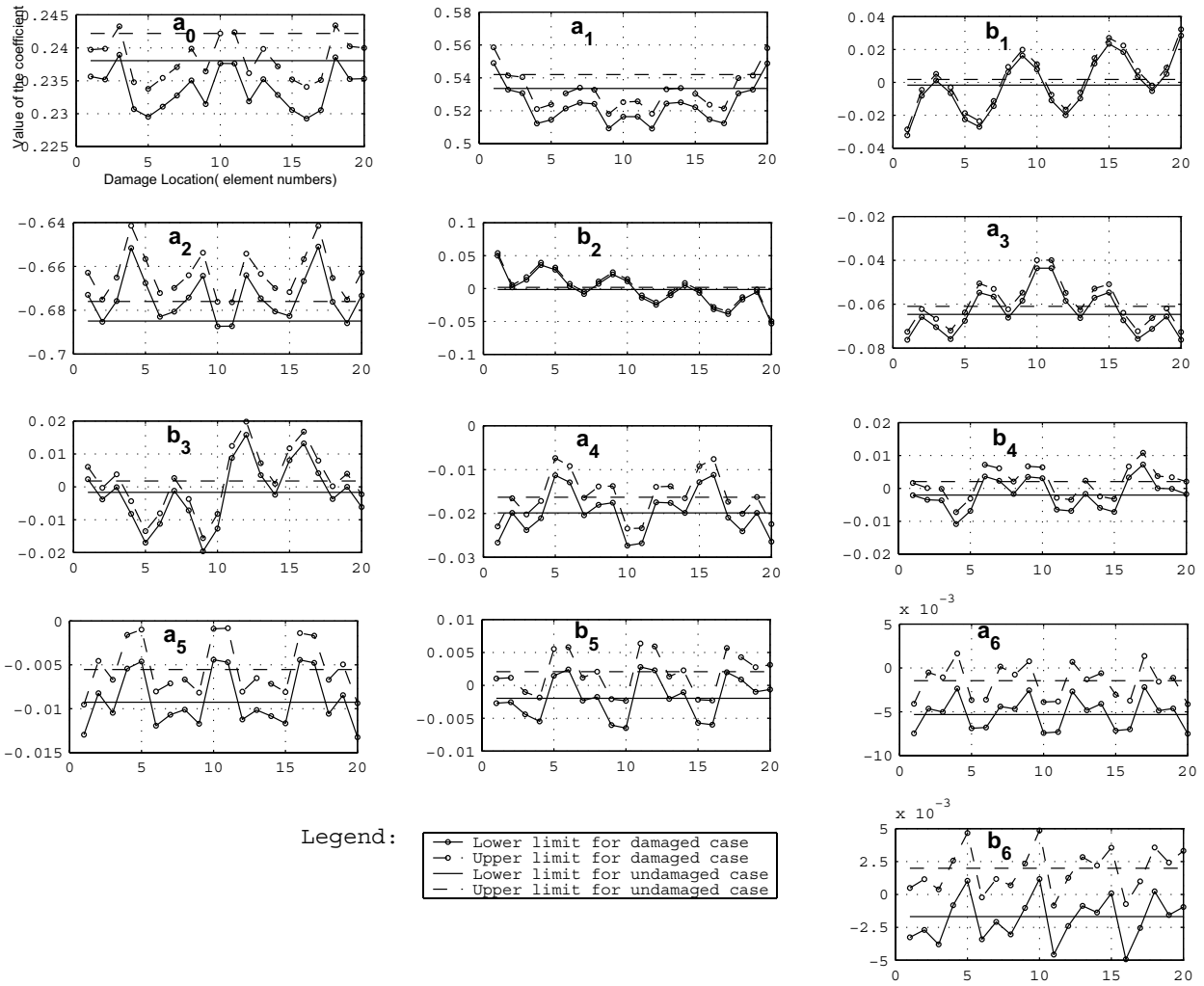

Figure 8: Variation of Fourier coefficients in presence of noise for 3^{rd} mode of fixed-fixed beam for undamaged and damage size of 40%

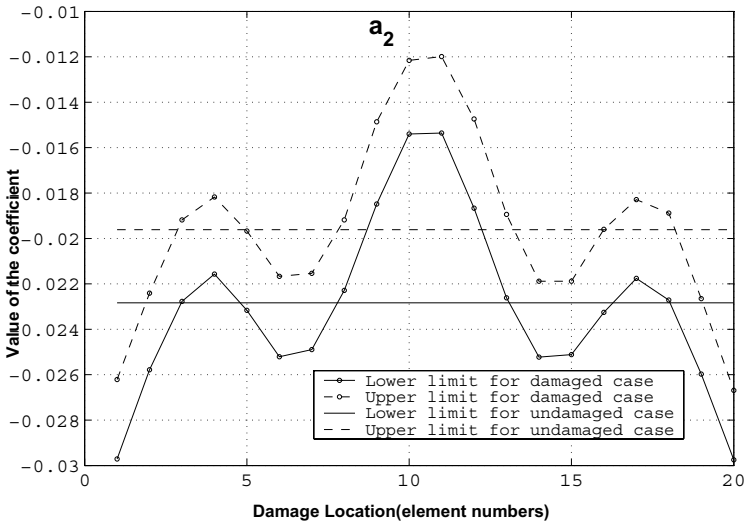

Figure 9: Variation of a_2 for the 1^{st} mode of a fixed-fixed beam

damage detection. In fact, these tables provide a rule base for the development of an expert system or fuzzy logic system.

It should be noted that the accuracy of measured mode shapes continues to improve due to advances in measuring and signal processing technology. Therefore, the method discussed in this paper can be used for damage detection of realistic beam type structures. In addition, though this paper has focussed on the fixed-fixed beam, the method is also applicable to fixed-pinned and pinned-pinned beams which are also spatially periodic.

7 Conclusions

A new method for damage detection and isolation using damage index in the form of a vector of sensitive Fourier coefficients for each damage size and location for beams fixed at both ends is developed in this paper. The method uses Fourier analysis of mode shapes in the spatial domain. Finite element analysis of a damaged beam is used to study the effect of damage location and size on spatial Fourier coefficients. It is found that the Fourier coefficients are sensitive to both damage size and location. In particular, the higher harmonic Fourier coefficients are quite sensitive to damage location. The Fourier coefficients of the first three modes can be used to isolate moderate levels of damage in the beam even in the presence of noise in the mode shapes. The Fourier coefficients in the spatial domain can therefore be used as damage indicators for fixed-fixed beams.

References

Abdo M. A. -B. and Hori M., (2002). A Numerical Study Of Structural Damage Detection Using Changes In The Rotation Of Mode Shapes. *Journal of Sound And Vibration* 251(2), 227-239.

Chang Ch. and Lien-Wen Ch., (2005). Detection Of The Location And Size Of Cracks In Multiple Cracked Beam By Spatial Wavelet Based Approch. *Mechanical Systems And Signal Processing* 19, 39-155.

Dimarogonas A. D., (1996). Vibration Of Cracked Structures: A State Of Art Review. *Engineering Fracture Mechanics* 55, 831-857.

Douka E., Loutridis S. and Trochidis A., (2003). Crack Identification Using Wavelet Analysis. *International Journal of Solids And Structures* 40, 3557-3569.

Farrar C. and Jauregui D., (1996). Damage Detection Algorithms Applied To Experimental And Numerical Modal Data From The I-40 Bridge. Technical Report La-13074-MS, Los Alamos National Laboratory.

Jeong-Tae K., Yeon-Sun R., Hyun-Man C., and Norris S., (2003). Damage identification in beam-type structures: frequency-based method vs mode-shape-based method. *Engineering Structures* 25(1), 57-67.

Khan A. Z., Stanbridge A. B. and Ewins D. J., (2000). Detecting Damage In Vibrating Structures With A Scanning LDV. *Optics And Lasers In Engineering* 32,538-592.

Lai J. Y. and Young K. F., (1995). Dynamics Of Graphite/Epoxy Composite Under Delamination Fracture And Environmental Effects. *Journal of Composite Structures* 30, 25-32.

Pandey A. K., Biswas M. Samman M. M., (1991). Damage Detection From Changes In Curvature Mode Shapes. *Journal of Sound And Vibration* 145(2), 321-332.

Pandey A. K. and Biswas M., (1994). Damage Detection In Structures Using Changes In Flexibility. *Journal Of Sound And Vibration* 169(1), 311-328.

Parloo P., Guillaume P. and Van Overmeire M., (2003). Damage Assessment Using Mode Shape Sensitivities. *Mechanical Systems And Signal Processing* 17(3), 499-518.

Peroni I., Paolzzi A. and Bramante A., (1991). Effect Of Debonding Damage On The Modal Damping Of A Sandwich Panel. Proceedings Of 9th International Modal Analysis Conference 2, 1617-1622.

Ratcliff. C. P., (1997). Damage Detection Using A Modified Laplacian Operator On Mode Shape Data. *Journal of Sound And Vibration*. 204(3), 505-517.

Ratcliff. C. P. and Bagaria, W. J., (1998). A Vibration Technique For Locating Delamination In Composite Beams. *AIAA J.* 36, no. 6, 1074-1077.

Rizos P. F. and Aspragathos N., (1990). Identification Of Crack Location And Magnitude In A Cantilever Beam From The Vibration Modes. *Journal of Sound And Vibration* 138(3), 381-388.

Salawu, O.S., (1997). Detection Of Structural Damage Through Changes In Frequency: A Review. *Engineering Structures* 19, 718-723.

Stubbs N., Kim J. T. and Topole K. G., (1992). An efficient And Robust Algorithm For Damage Localization In Offshore Platforms. ASCE 10th Structures Congress, 543-546.

Viola E., Federici L. and Nobile L., (2001). Detection Of Crack Location Using Cracked Beam Element Method For Structural Analysis. *Theoretical And Applied Fracture Mechanics* 36, 23-25.

Wang Q. and Deng X., (1999). Damage Detection With Spatial Wavelets. International *Journal of Solids And Structures* 36, 3443-3468.

Yoon M. K., Heider D., Gillespie J. W., Ratcliff. C. P. and Crane R. M., (2005). Local Damage Detection Using The Two-Dimensional Gapped Smoothing Method. *Journal of Sound And Vibration* 279, 119-139.

Zhang Z. and Aktan H. M., (1995). The Damage Indices For Constructed Facilities. Proceedings Of IMAC 13(2), 1520-1529.

Zimmerman D. C. and Kaou M., (1995). Structural Damage Detection Using A Minium Rank Update Theory. *ASME Journal Of Vibration And Acoustics* 116, 222-231.